Engineering Quantum Criticality for Quantum Dot Power Harvesting

Jin-Yi Wang(王金义)[1], Lei-Lei Nian(年磊磊)[1*], and Jing-Tao Lü(吕京涛)[2*]

[1]*School of Physics and Astronomy, Yunnan University, Kunming 650091, China*
[2]*School of Physics, Institute for Quantum Science and Engineering, and Wuhan National High Magnetic Field Center, Huazhong University of Science and Technology, Wuhan 430074, China*

(Received 20 December 2023; accepted manuscript online 18 January 2024)

Coupling of quantum-dot circuits to microwave photons enables us to investigate photon-assisted quantum transport. Here, we revisit this typical circuit quantum electrodynamical setup by introducing the Kerr nonlinearity of photons. By exploiting quantum critical behavior, we propose a powerful scheme to control the power-harvesting efficiency in the microwave regime, where the driven-dissipative optical system acts as an energy pump. It drives electron transport against a load in the quantum-dot circuit. The energy transfer and, consequently, the harvesting efficiency are enhanced near the critical point. As the critical point moves towards to low input power, high efficiency within experimental parameters is achieved. Our results complement fundamental studies of photon-to-electron conversion at the nanoscale and provide practical guidance for designs of integrated photoelectric devices through quantum criticality.

DOI: 10.1088/0256-307X/41/2/020503

In quantum statistical mechanics, phase transitions can be supported by a finite-size system with an infinite-dimensional Hilbert space. Naturally, phase transitions with a few bosonic degrees of freedom falls into this category. Driven dissipative optical systems have become one of the most important platforms for research of nonequilibrium quantum criticality[1–3] and offer promising applications in quantum metrology, quantum transducers, and other quantum technologies.[4–6]

Recently, hybrid systems in circuit quantum electrodynamics (cQED) setups, which couple an electronic circuit to a microwave cavity, have been actively studied.[7–12] On the one hand, for an equilibrium electronic circuit and driven cavity, photon-assisted electron transport can be used to control the photon-to-electron conversion.[13–18] On the other hand, a nonequilibrium electronic circuit, with the help of electron–photon coupling, can be used to engineer photon emission and to control the statistical properties of emitted photons, where antibunched, coherent, bunched, and superbunched photon emission has been studied.[19–25] Photonic quantum correlation can be established when the electronic circuit interacts with two or more cavities.[25,26] Moreover, power harvesting can be achieved when the electrons transport by absorbing cavity photons against an external voltage. The efficiency is defined as the ratio of the output power IV to input power $P_{\rm i}$, where I is the current flow against the voltage V. For a given V, a key challenge in the regulation of power harvesting is to enhance I at low $P_{\rm i}$.

It has been shown that quantum phase transition can even take place in a single Kerr resonator subject to single-photon driving,[27–33] where the photon excitation undergoes a jump process. Besides its scientific importance in nonequilibrium quantum many-body physics, the jump in cavity photon number during phase transition is particularly attractive for applications in quantum photovoltaics based on quantum-dot cQED.[34] This extends the cQED tasks in terms of photon-to-electron conversion by employing the advantages of quantum criticality. However, so far, a general framework for whether and how this scheme can be applied to power harvesting is lacking.

In this Letter, to address this issue, we introduce photon criticality as a potential tool to control power harvesting in a biased quantum dot cQED setup. We first propose a general mechanism for electron transport against a load and then provide an analytical expression for the current that enables us to examine the harvesting efficiency when the photon criticality is observed. Our theory, backed by numerics, indicates that the power output and efficiency are enhanced near the critical point where the energy exchange between photon and electron becomes more effective.

Very recently, microwave power harvesting has been experimentally reported in a linear resonator coupled to a double-quantum-dot (DQD) photodiode.[35] Our proposal of using quantum criticality has two main advantages. First, power harvesting efficiency can be optimized by only switching the critical point from high to low input power. Second, this protocol relies on photonic degrees of freedom, so it is robust against electronic dephasing and relaxation, which, in principle, can be generalized to multilevel systems with multi-photon absorption.[36–38] In experiments, driven-dissipative Kerr resonators have proved to be ideal candidates for realizing quantum phase transition.[29,31,32,39–42] When such systems are capacitively coupled to a quantum dot system, our proposal is well within reach.[15,18,35]

A tunnel-coupled DQD system coupled to a drive-

*Corresponding authors. Email: llnian@ynu.edu.cn; jtlu@hust.edu.cn
© 2024 Chinese Physical Society and IOP Publishing Ltd

dissipative Kerr resonator can be described by a Hamiltonian in the form of $H = H_{\rm s}(t) + H_{\rm e} + H_{\rm b}$. The term $H_{\rm s}(t)$ describes the DQD–resonator system

$$H_{\rm s}(t) = \frac{\varepsilon_{\rm d}}{2}\sigma_z + t_{\rm d}\sigma_x + \omega_{\rm r}a_{\rm r}^\dagger a_{\rm r} + g_{\rm r}\sigma_z(a_{\rm r}^\dagger + a_{\rm r}) + \frac{U_{\rm r}}{2}a_{\rm r}^\dagger a_{\rm r}^\dagger a_{\rm r}a_{\rm r} + 2\cos(\omega_{\rm L}t)\sqrt{\kappa_{\rm L}\dot{N}_{\rm L}}(a_{\rm r}^\dagger + a_{\rm r}), \quad (1)$$

where $\varepsilon_{\rm d}$ and $t_{\rm d}$ are the energy space and tunnel amplitude between two dot levels L and R; $\sigma_z = |{\rm L}\rangle\langle{\rm L}| - |{\rm R}\rangle\langle{\rm R}|$ and $\sigma_x = |{\rm L}\rangle\langle{\rm R}| + |{\rm R}\rangle\langle{\rm L}|$ are the Pauli matrices of the z and x components; $a_{\rm r}^\dagger$ ($a_{\rm r}$) is the creation (annihilation) operator of a photon with angular frequency $\omega_{\rm r}$ in the resonator. The DQD is capacitively coupled to the resonator via a longitudinal form with strength $g_{\rm r}$. The photons in the resonator feel the on-site repulsive interaction, $U_{\rm r}$, which describes the Kerr nonlinearity. The resonator is driven by a coherent classical field with frequency $\omega_{\rm L}$ and strength $\sqrt{\kappa_{\rm L}\dot{N}_{\rm L}}$, where $\kappa_{\rm L}$ and $\dot{N}_{\rm L}$ are the field–resonator coupling and incoming photon rate. The second term in H is the electrode Hamiltonian and its coupling with the dots, $H_{\rm e} = \sum_{k;v={\rm L,R}}(\varepsilon_{kv}c_{kv}^\dagger c_{kv} + t_{kv}c_{kv}^\dagger d_v + {\rm H.c.})$, where $c_{kv}^\dagger$ (c_{kv}) creates (annihilates) an electron of energy ε_{kv} with wave number k in the electrode v. The tunneling amplitude between the dot and its respective electrode is t_{kv}. The last term in Hamiltonian H, $H_{\rm b} = \sum_\alpha \omega_\alpha b_\alpha^\dagger b_\alpha + \sum_\alpha(t_{\alpha{\rm r}}b_\alpha^\dagger a_{\rm r} + t_{\alpha{\rm r}}^* b_\alpha a_{\rm r}^\dagger)$, describes the bath and its coupling with the resonator; $t_{\alpha{\rm r}}$ is the bath–resonator coupling strength.

For $\varepsilon_{\rm d} < 0$, the DQD Hamiltonian can be diagonalized by a unitary transformation as follows:

$$|g\rangle = \cos(\theta/2)|{\rm L}\rangle - \sin(\theta/2)|{\rm R}\rangle,$$
$$|e\rangle = \sin(\theta/2)|{\rm L}\rangle + \cos(\theta/2)|{\rm R}\rangle, \quad (2)$$

where $|g\rangle$ and $|e\rangle$ are the ground and excited states of the DQD with the energy space $\Omega_{\rm d} = \sqrt{\varepsilon_{\rm d}^2 + 4t_{\rm d}^2}$ and $\theta = \arctan(-2t_{\rm d}/\varepsilon_{\rm d})$. In a rotating frame, the dynamics of the DQD–resonator system is governed by the Lindblad master equation [43–45]

$$\frac{d}{dt}\rho(t) = -i[\mathcal{H}_{\rm s}, \rho(t)] + \mathcal{L}_{\rm e}[\rho(t)] + \mathcal{L}_{\rm b}[\rho(t)], \quad (3)$$

where the $\rho(t)$ reduced density matrix of the system and its coherent evolution are determined by the Hamiltonian in the rotating-wave approximation:

$$\mathcal{H}_{\rm s} = \frac{\Delta_{\rm d}}{2}\widetilde{\sigma}_z + \Delta_{\rm r}a_{\rm r}^\dagger a_{\rm r} + g_{\rm r}\sin\theta\,(a_{\rm r}\widetilde{\sigma}_+ + a_{\rm r}^\dagger\widetilde{\sigma}_-) + \frac{U_{\rm r}}{2}a_{\rm r}^\dagger a_{\rm r}^\dagger a_{\rm r}a_{\rm r} + \sqrt{\kappa_{\rm L}\dot{N}_{\rm L}}(a_{\rm r} + a_{\rm r}^\dagger), \quad (4)$$

where $\widetilde{\sigma}_z = |e\rangle\langle e| - |g\rangle\langle g|$ and $\widetilde{\sigma}_+ = (\widetilde{\sigma}_-)^\dagger = |e\rangle\langle g|$, $\Delta_{\rm d} = \Omega_{\rm d} - \omega_{\rm L}$ and $\Delta_{\rm r} = \omega_{\rm r} - \omega_{\rm L}$ are the frequency detunings. The electronic superoperator in Eq. (3) describes the tunneling processes between the dots and electrodes, $\mathcal{L}_{\rm e}[\rho(t)] = \sum_{v={\rm L,R}}\mathcal{L}_v[\rho(t)] = \sum_{v;i={\rm e,g}}\Gamma_{vi}^\theta\{f_v(\varepsilon_i)\mathcal{L}[|i\rangle\langle 0|, \rho(t)] + (1 - f_v(\varepsilon_i))\mathcal{L}[|0\rangle\langle i|, \rho(t)]\}$, where $f_v(\varepsilon) = [\exp((\varepsilon - \mu_v)/k_{\rm B}T) + 1]^{-1}$ with chemical potential μ_v and temperature T. The tunneling rates are $\Gamma_{\rm Le}^\theta = \Gamma_{\rm L}\Theta$, $\Gamma_{\rm Lg}^\theta = \Gamma_{\rm L}(1 - \Theta)$, $\Gamma_{\rm Rg}^\theta = \Gamma_{\rm R}\Theta$, and $\Gamma_{\rm Re}^\theta = \Gamma_{\rm R}(1 - \Theta)$ with $\Theta = \sin^2(\theta/2)$. For $\varepsilon_{\rm d} > 0$, $\Theta = \cos^2(\theta/2)$. The photonic superoperator in Eq. (3) describes the DQD–resonator energy exchange, $\mathcal{L}_{\rm b}[\rho(t)] = \kappa_{\rm r}\{n_{\rm B}(\omega_{\rm r})\mathcal{L}[a_{\rm r}^\dagger, \rho(t)] + (1 + n_{\rm B}(\omega_{\rm r}))\mathcal{L}[a_{\rm r}, \rho(t)]\}$, where $n_{\rm B}(\omega) = [\exp(\hbar\omega/k_{\rm B}T) - 1]^{-1}$ is the Bose–Einstein distribution and $\kappa_{\rm r}$ is the damping rate. The superoperator acting on $\rho(t)$ is given by $\mathcal{L}[\mathcal{O}, \rho(t)] = \mathcal{O}\rho(t)\mathcal{O}^\dagger - (\mathcal{O}^\dagger\mathcal{O}\rho(t) + \rho(t)\mathcal{O}^\dagger\mathcal{O})/2$ with a system operator $\mathcal{O}$.

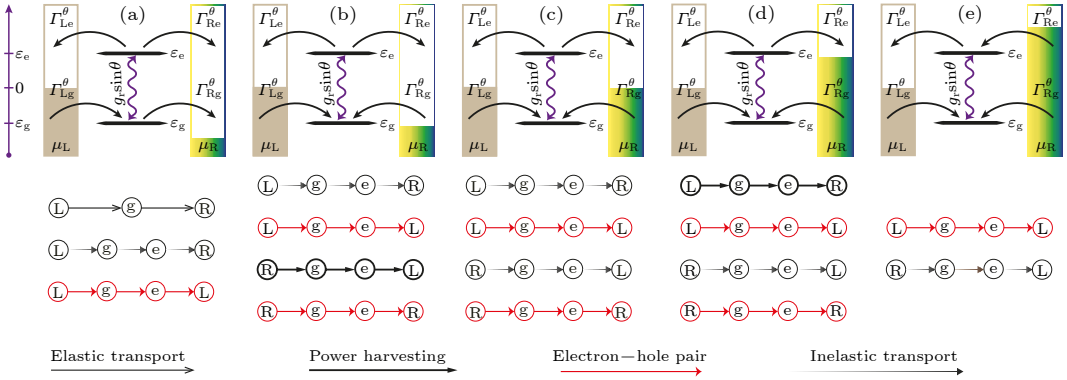

Fig. 1. Schematic of photon-mediated electron transport processes for $\mu_{\rm L} = 0$. Upper: the direction of the electron tunneling. Lower: the tunneling path.

We first analyze the mechanism of the power harvesting, where the DQD system is set to harvest photons from the driven-dissipative resonator. When $\mu_{\rm L} = 0$ and $T \approx 0$, five different electron tunneling processes depending on $\mu_{\rm R}$ are summarized in Fig. 1. For $\mu_{\rm R} < \varepsilon_{\rm g}$ in Fig. 1(a), an electron from the left electrode enters into level g, it can then tunnel to the right electrode directly. With the absorption of a photon, two tunneling channels from level e to left and right electrodes are open, and the former is the process for electron–hole pair creation. For $\mu_{\rm R} > \varepsilon_{\rm g}$, the level g is occupied by an electron from one electrode, it tunnels to level e by absorbing a photon and then to another electrode or back to the same one. The electron–hole pair is created when donor and acceptor of the electron is the same electrode. When the electron transport through two different electrodes, the photon-assisted electron transport occurs for $\varepsilon_{\rm g} < \mu_{\rm R} = 0$ [Fig. 1(c)]; while for $0 > \mu_{\rm R} > \varepsilon_{\rm g}$ and $\varepsilon_{\rm e} > \mu_{\rm R} > 0$, the electron can transport opposite to an external voltage, then the power harvesting is observed [Figs. 1(b) and 1(d)]. For $\mu_{\rm R} > \varepsilon_{\rm e}$, an electron tunnels into

level g from the right electrode, it can absorb a photon and tunnel out from level e [Fig. 1(e)]. We would like to make clear that, for energy harvesting, the DQD absorbs energy from the environment, such as phonons, photons, and magnons.[46–54]

It has been demonstrated that the coherent driven and dissipative nonlinear resonator yields the phase transition, where the competition between drive, nonlinearity and dissipation leads to a photon jump.[27–33] When the DQD system is in equilibrium, as shown in Fig. 1(c), such a jump behavior has been used to enhance the photovoltaic current.[34] In the microwave regime, power harvesting is observed experimentally in a DQD photodiode where the efficiency lies below 2%.[35] To optimize the efficiency of the power harvesting, we proceed to engineer a quantum criticality for the nonequilibrium cases in Figs. 1(b) and 1(d), where the electrons transport against a load.

We now assess the photon criticality and discuss the effects of the electronic degree of freedom. For $g_\mathrm{r} = 0$, the expectation value of a_r in the steady state is $\alpha_\mathrm{r} = i\sqrt{\kappa_\mathrm{L}\dot{N}_\mathrm{L}}/(-i\Delta_\mathrm{r} - iU_\mathrm{r}|\alpha_\mathrm{r}|^2 - \kappa_\mathrm{r}/2)$ with $\alpha_\mathrm{r} = \langle a_\mathrm{r}\rangle$, where the quantum fluctuations are ignored and the system evolves in a semiclassical way (Appendix A in the Supplemental Material). When $U_\mathrm{r} \neq 0$, two steady-state solutions may be predicted, while for $U_\mathrm{r} = 0$ only one is obtained.[28,55,56] With the quantum fluctuations, the system can undergo a metastable state where the photon density is equal to the average of the two semiclassical branches. The transition between the two branches become more and more sharper when the system gradually approaches the thermodynamic limit. For a well-defined thermodynamic limit, the photon density converges to one of the two branches, leading to the observation of a discontinuous jump and, consequently, a first-order phase transition. For $g_\mathrm{r} \neq 0$ and in the power harvesting regions, we have

$$\alpha_\mathrm{r} = \frac{i\sqrt{\kappa_\mathrm{L}\dot{N}_\mathrm{L}}}{-i\widetilde{\Delta}_\mathrm{r} - iU_\mathrm{r}\,|\alpha_\mathrm{r}|^2 - \widetilde{\kappa}_\mathrm{r}}, \tag{5}$$

where the detuning and dissipation become $\widetilde{\Delta}_\mathrm{r} = \Delta_\mathrm{r}(1 + 2\mathcal{E})$ and $\widetilde{\kappa}_\mathrm{r} = \kappa_\mathrm{r}/2 - \Gamma_\mathrm{R}\mathcal{E}$ with $\mathcal{E} = 2g_\mathrm{r}^2\sin^2\theta\langle\widetilde{\sigma}_z\rangle/(4\Delta_\mathrm{r}^2 + \Gamma_\mathrm{R}^2)$. Clearly, two steady-state solutions may also be achieved and thus the photon criticality survives.

In turn, we give the contribution to the current due to the photon criticality. For $\Gamma_\mathrm{L} = \Gamma_\mathrm{R}$, the steady-state current flowing from the right electrode is given as follows:

$$I_\mathrm{R} = \begin{cases} -e\,[\Theta(1-\Theta)\Gamma_\mathrm{R} + \mathcal{C}(1 - 3\Theta + \Theta^2)], & \mu_\mathrm{R} < \varepsilon_\mathrm{g}, \\ -e\,\mathcal{C}(1-2\Theta), & \varepsilon_\mathrm{g} < \mu_\mathrm{R} < \varepsilon_\mathrm{e}, \\ e\,\mathcal{C}, & \mu_\mathrm{R} > \varepsilon_\mathrm{e}, \end{cases} \tag{6}$$

$$\mathcal{C} = -i\Big[\sqrt{\kappa_\mathrm{L}\dot{N}_\mathrm{L}}(\langle a_\mathrm{r}^\dagger\rangle - \langle a_\mathrm{r}\rangle)\Big] - \kappa_\mathrm{r}\langle a_\mathrm{r}^\dagger a_\mathrm{r}\rangle, \tag{7}$$

where $\mathcal{C}$ describes the average photon excitation for the momentum and occupation (Appendix B in the Supplemental Material); $e > 0$ is the elementary charge. For $\mu_\mathrm{R} < \varepsilon_\mathrm{g}$, the electron transport is mediated by an elastic channel, while for $\mu_\mathrm{R} > \varepsilon_\mathrm{g}$ the electron can only tunnel in an inelastic way. It is clear that the photon criticality is manifested in the current exhibiting a jump, especially when power harvesting occurs [Figs. 1(b) and 1(d)]. We can then define the power output and the efficiency, respectively, as

$$P_\mathrm{o} = \sum_{v=\mathrm{L,R}} \mu_v \mathrm{Tr}\{Q\mathcal{L}_v[\rho(\infty)]\} = \frac{(\mu_\mathrm{R} - \mu_\mathrm{L})I_\mathrm{R}}{e}, \tag{8}$$

$$\eta = -\frac{P_\mathrm{o}}{P_\mathrm{i}}, \tag{9}$$

where $Q = |e\rangle\langle e| + |g\rangle\langle g|$ is the number operator and $P_\mathrm{i} = \hbar\omega_\mathrm{r}\dot{N}_\mathrm{L}$ is the input power. From the first law of thermodynamics, the power output is equivalent to the sum of energy fluxes flowing through the DQD; that is, $P_\mathrm{o} = -(J_\mathrm{L} + J_\mathrm{R} + J_\mathrm{p})$, where $J_v = \mathrm{Tr}\{(H_\mathrm{d} - \mu_v Q)\mathcal{L}_v[\rho(\infty)]\}$ and $J_\mathrm{p} = -\mathrm{Tr}\{i[H_\mathrm{d}, \mathcal{H}_\mathrm{s}]\rho(\infty)\}$ (Appendix C in the Supplemental Material). H_d is the Hamiltonian of the DQD.

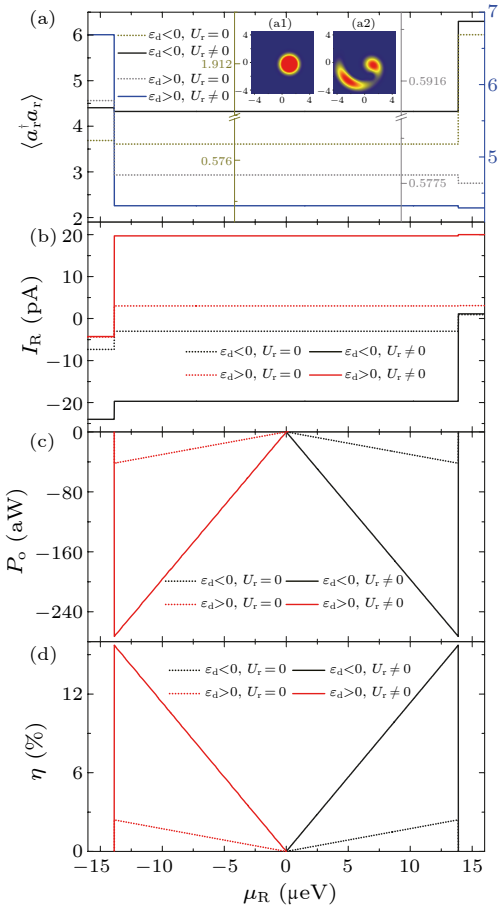

Fig. 2. Chemical potential dependence of mean photon number $\langle a_\mathrm{r}^\dagger a_\mathrm{r}\rangle$ (a), current I_R (b), power output P_o (c), and efficiency η (d). The dashed and solid lines correspond to $U_\mathrm{r} = 0$ and $U_\mathrm{r} = 25\,\mathrm{MHz}$. The inset in (a) exhibits the Wigner functions for $U_\mathrm{r} = 0$ (a1) and $U_\mathrm{r} = 25\,\mathrm{MHz}$ (a2) at $\mu_\mathrm{R} = 13.87\,\mu\mathrm{eV}$ and $\varepsilon_\mathrm{d} = -27.3\,\mu\mathrm{eV}$. The other parameters are $\mu_\mathrm{L} = 0$, $\Gamma_\mathrm{L}/2\pi = \Gamma_\mathrm{R}/2\pi = 540\,\mathrm{MHz}$, $g_\mathrm{r}/2\pi = 149.87\,\mathrm{MHz}$, $\kappa_\mathrm{r} = 25\,\mathrm{MHz}$, $\kappa_\mathrm{L}/2\pi = 3.8\,\mathrm{MHz}$, $\dot{N}_\mathrm{L} = 391\,\mathrm{MHz}$, $t_\mathrm{d} = 2.5\,\mu\mathrm{eV}$, $\omega_\mathrm{r} = \Omega_\mathrm{d}$, $\omega_\mathrm{L} = \Omega_\mathrm{d} + 5\kappa_\mathrm{r}$, and $P_\mathrm{i} = 1.74\,\mathrm{fW}$. The parameters are extracted from relevant experiments.[35,57,58]

To realize our prediction, the crucial parameters that relate θ to I_R and $\langle a_\mathrm{r}^\dagger a_\mathrm{r}\rangle$ are t_d and ε_d, which can be cho-

sen experimentally so as to achieve $\tan^2(\theta/2) < 1$ for both $\varepsilon_{\rm d} < 0$ and $\varepsilon_{\rm d} > 0$. By changing the input power $P_{\rm i}$, the critical point of photon excitation and current can be extracted (Appendix D in the Supplemental Material). Near the critical point, we plot in Fig. 2(a) the mean photon number $\langle a_{\rm r}^\dagger a_{\rm r}\rangle$ as a function of the chemical potential $\mu_{\rm R}$ for indicated $U_{\rm r}$. In the region of power harvesting, a finite $U_{\rm r}$ leads to the enhancement of $\langle a_{\rm r}^\dagger a_{\rm r}\rangle$ for both $\varepsilon_{\rm d} < 0$ and $\varepsilon_{\rm d} > 0$. In the inset, the Winger functions for $\varepsilon_{\rm d} < 0$ are shown (as the same as those for $\varepsilon_{\rm d} > 0$ in Fig. S1), and a single peak is found for $U_{\rm r} = 0$, while a bimodal shape induced by optical bistability appears for $U_{\rm r} \neq 0$, similarly for $\varepsilon_{\rm d} > 0$. Thus, the enhanced $\langle a_{\rm r}^\dagger a_{\rm r}\rangle$ is caused by the presence of the first-order quantum phase transition. Chemical potential dependence of the current $I_{\rm R}$ is shown in Fig. 2(b), where two features are worth mentioning. First, for $\varepsilon_{\rm d} < 0$, the electron injected from the left electrode occupies level g, then the photon pumps it to level e and subsequently to the right electrode, see Fig. 1(d). Therefore, the electron tunnels from the left to the right electrode by absorbing a photon, yielding transport against voltage and thus power harvesting; that is, $I_{\rm R} < 0$ for $\mu_{\rm R} > 0$. A similar transport process to that in Fig. 1(b) can be achieved for $\varepsilon_{\rm d} > 0$, where $I_{\rm R} > 0$ for $\mu_{\rm R} < 0$ is observed. Second, the current for a finite $U_{\rm r}$ is considerably enhanced at $\mu_{\rm R} = \pm 13.87\,\mu$eV. Physically, the energy exchange between the DQD and the resonator leads to $J_{\rm p} \propto I_{\rm R}$, thus the enhanced current is induced by the increased energy transfer from the photon to the electron system. As is expected, the power harvesting effect is optimized at the critical point, which is reflected by enhanced values of the power output $P_{\rm o}$ and the efficiency η in Figs. 2(c) and 2(d). Note that our results do not depend on $\mu_{\rm L}$ (Appendix E in the Supplemental Material).

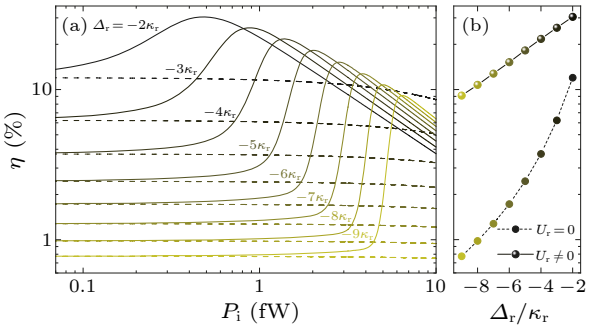

Fig. 3. (a) Efficiency η as a function of input power $P_{\rm i}$ for different detunings $\Delta_{\rm r}$ at $\varepsilon_{\rm d} = -27.3\,\mu$eV and $\mu_{\rm R} = 13.87\,\mu$eV. (b) Maximum value of efficiency η in (a). The other parameters are the same as those in Fig. 2.

According to Eq. (9), one may expect high efficiency at low input power. For low $P_{\rm i}$, the electron tends to stay at level g and thus $\langle\widetilde{\sigma}_z\rangle \approx -1$ (Appendixes B and F in the Supplemental Material). When $U_{\rm r} = 0$, the quantum fluctuations may be ignored. Then, the efficiency can be approximated by

$$\eta \approx \frac{16\mu_{\rm R}\kappa_{\rm L}g_{\rm r}^2\sin^2\theta\cos\theta}{\hbar\omega_{\rm r}\Gamma_{\rm R}\left[4\Delta_{\rm r}^2\left(1-\frac{4g_{\rm r}^2\sin^2\theta}{\Gamma_{\rm R}^2}\right)^2+\left(\kappa_{\rm r}+\frac{4g_{\rm r}^2\sin^2\theta}{\Gamma_{\rm R}}\right)^2\right]}, \quad (10)$$

where the efficiency η is independent of the input power $P_{\rm i}$, resulting from the linearity in the $\eta - P_{\rm i}$ characteristic of the excitation. The maximum value of η at the low $P_{\rm i}$ increases with increasing $\Delta_{\rm r}$, which is in agreement with the numerical results in Figs. 3(a) and 3(b) (dashed lines). For $U_{\rm r} = 0$, Eq. (10) is a general form of measuring the power harvesting. In this case, we show the $\Delta_{\rm r}$-mediated η allowed by the control of the frequency $\omega_{\rm L}$, while the other parameters (e.g., $g_{\rm r}$ and $\kappa_{\rm r}$) cannot be flexibly adjusted. When $U_{\rm r} \neq 0$, not only does the photon criticality become active for electron transport, but the critical point moves towards lower $P_{\rm i}$ with increasing $\Delta_{\rm r}$. This critical shift is clearly visible in Eq. (5). Therefore, high efficiency at low input power is enabled, as indicated by the solid lines in Figs. 3(a) and 3(b).

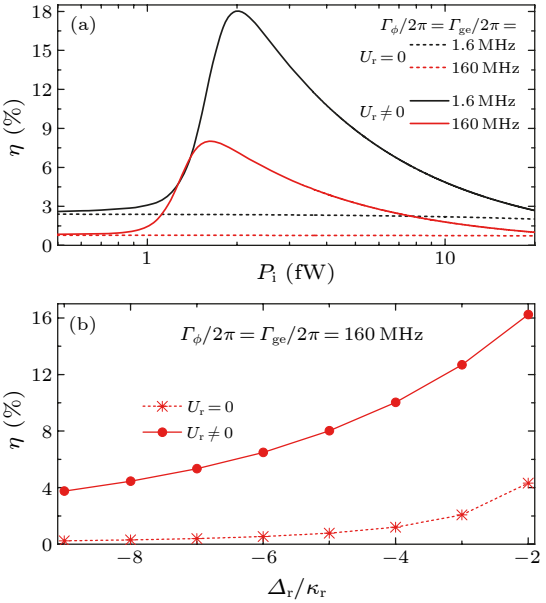

Fig. 4. (a) Efficiency η as a function of the input power $P_{\rm i}$ for indicated values of $U_{\rm r}$ in the presence of the electronic dephasing and relaxation. (b) Maximum value of efficiency η in (a). The other parameters are the same as those in Fig. 3.

To assess the feasibility of engineering photon criticality for efficiency enhancement, it is necessary to consider the effect of electronic dephasing and relaxation of the DQD. Inserting $\Gamma_\phi\mathcal{L}[\widetilde{\sigma}_z, \rho(t)]$ and $\Gamma_{\rm ge}\mathcal{L}[\widetilde{\sigma}_-, \rho(t)]$ into Eq. (3) with $\langle\widetilde{\sigma}_z\rangle \approx -1$ (Appendixes F and G in the Supplemental Material), one obtains the steady-state efficiency

$$\eta \approx \frac{\mu_{\rm R}\mathcal{C}_{\rm d2}^a\Gamma_{\rm R}\cos\theta}{(\Gamma_{\rm R}+\Gamma_{\rm ge})P_{\rm i}}, \quad (11)$$

with the photon excitation

$$\begin{aligned}\mathcal{C}_{\rm d2}^a = \Big[&\sqrt{\kappa_{\rm L}\dot{N}_{\rm L}}\Big(2i\widetilde{\Delta}_{\rm r2}U_{\rm r}\,{\rm Im}\langle a_{\rm r}^\dagger a_{\rm r}^\dagger a_{\rm r}\rangle \\ &+ 2\widetilde{\kappa}_{\rm r2}U_{\rm r}\,{\rm Re}\langle a_{\rm r}^\dagger a_{\rm r}^\dagger a_{\rm r}\rangle \\ &+ 2\widetilde{\kappa}_{\rm r2}\sqrt{\kappa_{\rm L}\dot{N}_{\rm L}}\Big)\Big](\widetilde{\Delta}_{\rm r2}^2+\widetilde{\kappa}_{\rm r2}^2)^{-1} - \kappa_{\rm r}\langle a_{\rm r}^\dagger a_{\rm r}\rangle, \quad (12)\end{aligned}$$

and the renormalized detuning and dissipation $\widetilde{\Delta}_{\rm r2} = \Delta_{\rm r}(1-\mathcal{E}_{\rm d})$ and $\widetilde{\kappa}_{\rm r2} = \kappa_{\rm r}/2 + \mathcal{E}_{\rm d}\mathcal{D}_2$ with $\mathcal{E}_{\rm d} = g_{\rm r}^2\sin^2\theta/(\Delta_{\rm r}^2+$

$\mathcal{D}_2^2$) and $\mathcal{D}_2 = 2\Gamma_\phi + \Gamma_{\rm ge}/2 + \Gamma_{\rm R}/2$. The photon dependence of the efficiency normalized by the effective coupling $\Gamma_{\rm R}/(\Gamma_{\rm R} + \Gamma_{\rm ge})$, which is presented in Eq. (11), is generally similar to that of the one given by Eqs. (6)–(9). The $P_{\rm i}$ dependence of η at $\Delta_{\rm r} = -5\kappa_{\rm r}$ is shown in Fig. 4(a). One important consequence of the presence of Γ_ϕ and $\Gamma_{\rm ge}$ is the suppression of η for both $U_{\rm r} = 0$ and $U_{\rm r} \neq 0$. In the experiment, a semiconductor DQD may give $\Gamma_\phi/2\pi = \Gamma_{\rm ge}/2\pi \approx 160\,{\rm MHz}$,[59] where it leads to a significant decrease of η. Interestingly, η increases with increasing $\Delta_{\rm r}$ [Fig. 4(b)], which occurs due to enhanced current in the low $P_{\rm i}$, as mentioned in Fig. 3(b).

In conclusion, we reveal the influence of photon criticality on the power harvesting of a DQD system coupled to a microwave resonator with Kerr nonlinearity. Harvesting efficiency is enhanced significantly near the critical point due to the efficient energy exchange from the photon to the electron system. Shifting the critical point to a low input power can further optimize the efficiency, which remains robust against electronic dephasing and relaxation. Our results open up the possibility of engineering photon criticality for efficient power harvesting and provide significant insights into bridging photon-to-electron conversion with quantum criticality.

Acknowledgements. This work was supported by the National Natural Science Foundation of China (Grant Nos. 12204405, 21873033, and 22273029), and the Yunnan Fundamental Research Project (Grant Nos. 202301AT070108 and 202401AW070005).

References

[1] Carusotto I and Ciuti C 2013 *Rev. Mod. Phys.* **85** 299
[2] Sieberer L M, Buchhold M, and Diehl S 2016 *Rep. Prog. Phys.* **79** 096001
[3] Noh C and Angelakis D G 2017 *Rep. Prog. Phys.* **80** 016401
[4] Garbe L, Bina M, Keller A, Paris M G, and Felicetti S 2020 *Phys. Rev. Lett.* **124** 120504
[5] Heugel T L, Biondi M, Zilberberg O, and Chitra R 2019 *Phys. Rev. Lett.* **123** 173601
[6] Casteels W and Ciuti C 2017 *Phys. Rev. A* **95** 013812
[7] Kurizki G, Bertet P, Kubo Y, Mølmer K, Petrosyan D, Rabl P, and Schmiedmayer J 2015 *Proc. Natl. Acad. Sci. USA* **112** 3866
[8] Gudmundsson V, Sitek A, Lin P Y, Abdullah N R, Tang C S, and Manolescu A 2015 *ACS Photon.* **2** 930
[9] Abdullah N R, Tang C S, Manolescu A, and Gudmundsson V 2016 *ACS Photon.* **3** 249
[10] Viennot J J *et al.* 2016 *C. R. Phys.* **17** 705
[11] Lu J, Wang R, Ren J, Kulkarni M, and Jiang J H 2019 *Phys. Rev. B* **99** 035129
[12] Blais A, Grimsmo A L, Girvin S M, and Wallraff A 2021 *Rev. Mod. Phys.* **93** 025005
[13] Xu C and Vavilov M G 2013 *Phys. Rev. B* **87** 035429
[14] Wong C H and Vavilov M G 2017 *Phys. Rev. A* **95** 012325
[15] Khan W *et al.* 2021 *Nat. Commun.* **12** 5130
[16] Ghirri A, Cornia S, and Affronte M 2020 *Sensors* **20** 4010
[17] Zenelaj D, Potts P P, and Samuelsson P 2022 *Phys. Rev. B* **106** 205135
[18] Haldar S, Havir H, Khan W, Lehmann S, Thelander C, Dick K A, and Maisi V F 2023 *Phys. Rev. Lett.* **130** 087003
[19] Lambert N, Nori F, and Flindt C 2015 *Phys. Rev. Lett.* **115** 216803
[20] Rastelli G and Governale M 2019 *Phys. Rev. B* **100** 085435
[21] Mantovani M, Armour A D, Belzig W, and Rastelli G 2019 *Phys. Rev. B* **99** 045442
[22] Schaeverbeke Q, Avriller R, Frederiksen T, and Pistolesi F 2019 *Phys. Rev. Lett.* **123** 246601
[23] Nian L L, Wang T, Zhang Z Q, Wang J S, and Lü J T 2020 *J. Phys. Chem. Lett.* **11** 8721
[24] Avriller R, Schaeverbeke Q, Frederiksen T, and Pistolesi F 2021 *Phys. Rev. B* **104** L241403
[25] Nian L L, Zheng B, and Lü J T 2023 *Phys. Rev. B* **107** L241405
[26] Hellbach F, Pauly F, Belzig W, and Rastelli G 2022 *Phys. Rev. B* **105** L241407
[27] Bartolo N, Minganti F, Casteels W, and Ciuti C 2016 *Phys. Rev. A* **94** 033841
[28] Casteels W, Fazio R, and Ciuti C 2017 *Phys. Rev. A* **95** 012128
[29] Rodriguez S, Casteels W, Storme F, Zambon N C, Sagnes I, Gratiet L L, Galopin E, Lemaître A, Amo A, Ciuti C, and Bloch J 2017 *Phys. Rev. Lett.* **118** 247402
[30] Minganti F, Biella A, Bartolo N, and Ciuti C 2018 *Phys. Rev. A* **98** 042118
[31] Fink T, Schade A, Höfling S, Schneider C, and Imamoglu A 2018 *Nat. Phys.* **14** 365
[32] Brookes P, Tancredi G, Patterson A D, Rahamim J, Esposito M, Mavrogordatos T K, Leek P J, Ginossar E, and Szymanska M H 2021 *Sci. Adv.* **7** eabe9492
[33] Kewming M J, Mitchison M T, and Landi G T 2022 *Phys. Rev. A* **106** 033707
[34] Nian L L, Hu S, Xiong L, Lü J T, and Zheng B 2023 *Phys. Rev. B* **108** 085430
[35] Haldar S, Zenelaj D, Potts P P, Havir H, Lehmann S, Dick K A, Samuelsson P, and Maisi V F 2023 arXiv:2306.15797 [cond-mat.mes-hall]
[36] Scully M O, Chapin K R, Dorfman K E, Kim M B, and Svidzinsky A 2011 *Proc. Natl Acad. Sci. USA* **108** 15097
[37] Creatore C, Parker M A, Emmott S, and Chin A W 2013 *Phys. Rev. Lett.* **111** 253601
[38] Zhao S C and Chen J Y 2019 *New J. Phys.* **21** 103015
[39] Geng Z, Peters K, Trichet A, Malmir K, Kolkowski R, Smith J, and Rodriguez S 2020 *Phys. Rev. Lett.* **124** 153603
[40] Chen Q M, Fischer M, Nojiri Y, Renger M, Xie E, Partanen M, Pogorzalek S, Fedorov K G, Marx A, Deppe F, and Rudolf G 2023 *Nat. Commun.* **14** 2896
[41] Roy A, Nehra R, Langrock C, Fejer M, and Marandi A 2023 *Nat. Phys.* **19** 427
[42] Beaulieu G, Minganti F, Frasca S, Savona V, Felicetti S, Di Candia R, and Scarlino P 2023 arXiv:2310.13636 [quant-ph]
[43] Lindblad G 1976 *Commun. Math. Phys.* **48** 119
[44] Breuer H P and Petruccione F 2002 *The Theory of Open Quantum Systems* (Oxford: Oxford University Press)
[45] Carmichael H J 2013 *Statistical Methods in Quantum Optics 1: Master Equations and Fokker-Planck Equations* (Berlin: Springer)
[46] Schmidt D, Schoelkopf R, and Cleland A 2004 *Phys. Rev. Lett.* **93** 045901
[47] Entin-Wohlman O, Imry Y, and Aharony A 2010 *Phys. Rev. B* **82** 115314
[48] Sothmann B and Büttiker M 2012 *Europhys. Lett.* **99** 27001
[49] Jordan A N, Sothmann B, Sánchez R, and Büttiker M 2013 *Phys. Rev. B* **87** 075312
[50] Sothmann B, Sánchez R, and Jordan A N 2015 *Nanotechnology* **26** 032001
[51] Xi M, Wang R, Lu J, and Jiang J H 2021 *Chin. Phys. Lett.* **38** 088801
[52] Wang R, Wang C, Lu J, and Jiang J H 2022 *Adv. Phys. X* **7** 2082317
[53] Lu J, Wang Z, Peng J, Wang C, Jiang J H, and Ren J 2022 *Phys. Rev. B* **105** 115428
[54] Ren J 2023 *Chin. Phys. Lett.* **40** 090501
[55] Drummond P and Walls D 1980 *J. Phys. A* **13** 725
[56] Kheruntsyan K 1999 *J. Opt. B* **1** 225
[57] Liu Y Y, Petersson K, Stehlik J, Taylor J M, and Petta J R 2014 *Phys. Rev. Lett.* **113** 036801
[58] Kulkarni M, Cotlet O, and Türeci H E 2014 *Phys. Rev. B* **90** 125402
[59] Hayashi T, Fujisawa T, Cheong H D, Jeong Y H, and Hirayama Y 2003 *Phys. Rev. Lett.* **91** 226804